Progress of Theoretical Physics, Vol. 76, No. 6, December 1986

Motion of a Shell at Metric Junction

Humitaka SATO

Department of Physics, Kyoto University, Kyoto 606

(Received July 19, 1986)

Motion of the spherical shell at metric junctions among the Minkowski, Schwarzschild and de Sitter metrics is investigated both for a dust shell and a vacuum energy shell. Using the positive energy condition for the shell, some junctions are excluded. Different junction leads to different self-energy or different expansion rate of the shell.

§ 1. Introduction

In 1966, Israel presented the general relativistic method to treat the motion of an infinitely thin shell or a singular layer.[1] Recently, the interest to this problem has revived through cosmological problems such as the GUT phase transtion in the early universe[2]~[5] and the void enlargement to form the large scale structure of galaxy distribution.[6],[7]

In a scenario of the vacuum phase transition, bubbles of the true vacuum are created in the false vacuum and the bubble expands forming a shell at the boundary. In Ref. 2), the motion of this shell was treated neglecting the effect of gravity. Recently, Berezin, Kuzmin and Tkachev have worked the general relativistic treatment of the bubble shell motion.[4],[5]

In 1983, Maeda and the present author investigated how the zero density spherical region expands in the expanding dust universe.[6],[7] This work was motivated by the discovery of the large void in the galaxy distribution. Our relativistic results were found to coincide with those obtained by the shock wave treatment,[8] in the Newtonian limit.

Main purpose of this paper is to present the mathematical analysis about the motion of shell at the metric junction among the Minkowski metric, the Schwarzschild metric and the de Sitter metric. We have found several results, which seem to be nontrivial at least intuitively. Further study of their physical implication is left for future. We also do not mention any application of these results.

In § 2, the basic formulation of Israel is given and the discussion by Berezin, Kuzmin and Tkachev[9] is also repeated. In § 3, possible junctions among the Minkowski metric, the Schwarzschild metric and the de Sitter metric are considered. In § 4, motion of a dust shell at the Minkowski-Schwarzschild junction and the Schwarzschild-Schwarzschild junction is studied. The effect of gravitational self-energy is clarified. In § 5, motion of a vacuum energy shell at various junctions among the Minkowski, Schwarzschild and de Sitter metrices is studied. In § 6, some discussions are given.

§ 2. Timelike hypersurface embedded in a given spacetime

We consider a hypersurface Σ which divides the 4-spacetime into two regions V^+ and V^-, whose metrics are written as

$$ds^2=g^{\pm}_{\mu\nu}dx^{\pm\mu}dx^{\pm\nu} \qquad (2\cdot1)$$

respectively with the sign $(+, -, -, -)$ and $\mu=0, 1, 2, 3$. Taking the normal vector to Σ as $\boldsymbol{n}$, the hypersurface Σ is called "timelike" if $\boldsymbol{n}\cdot\boldsymbol{n}<0$ and "spacelike" if $\boldsymbol{n}\cdot\boldsymbol{n}>0$. In the conventional (1+3)ADM formalism, the hypersurface is taken to be spacelike. In the present problem, however, we consider a timelike hypersurface and the metric on Σ can be introduced as

$$dl^2 = h_{ab} d\xi^a d\xi^b \, . \tag{2·2}$$

Using the Gauss-Codazzi relation, the Einstein tensor $G_{\mu\nu}$ is written in terms of extrinsic curvature K_{ab} and intrinsic curvature ${}^3R$ on Σ as

$$2G_{\mu\nu}n^\mu n^\nu = {}^3R - K_{ab}K^{ab} + K^2 \tag{2·3}$$

and

$$G_{\mu\nu}\tilde{h}_a{}^\mu n^\nu = K^b_{a|b} - K_{|a} \, , \tag{2·4}$$

where $K_{ab} = \tilde{h}_a{}^\mu \tilde{h}_b{}^\nu n_{\mu;\nu}$, $\tilde{h}_a{}^\mu = \partial x^\mu / \partial \xi^a$ on Σ and | denotes the covariant derivative in the space (2·2).

We introduce the Gauss coordinates in the neighbourhood of Σ in such a manner as

$$ds^2 = h_{ab} d\xi^a d\xi^b - dz^2 \tag{2·5}$$

with $z=0$ on Σ. Then, it is found that $\Gamma^z_{zz} = \Gamma^a_{zz} = \Gamma^z_{za} = 0$ on Σ. In this coordinate system, the Ricci tensor takes a form

$$R_{ab} = \frac{\partial \Gamma^z_{ab}}{\partial z} + (\Gamma^z_{ab}\Gamma^c_{zc} - 2\Gamma^c_{az}\Gamma^z_{cb} + {}^3R_{ab}) \, . \tag{2·6}$$

Substituting this relation into the Einstein equation $G_{\mu\nu} = -8\pi G T_{\mu\nu}$ and taking the integral over the Gauss coordinate through the infinitely thin shell, we get the relation

$$K^+_{ab} - K^-_{ab} = -8\pi G\left(S_{ab} - \frac{1}{2}h_{ab}S\right) \tag{2·7}$$

with

$$K^\pm_{ab} = \lim_{\Delta\to 0}\Gamma^z_{ab} = 2^{-1}(\partial h_{ab}/\partial z)_{\Sigma^\pm} \tag{2·8}$$

and

$$S_{ab} = \lim_{\Delta\to 0}\int_{-\Delta}^{\Delta} T_{ab}dz \, , \tag{2·9}$$

where we have used a boundedness of the bracket term in (2·6).

Substituting (2·3) and (2·4) into the Einstein equation and taking the difference of both sides of Σ, we get the following results:

$$S^{ab}\tilde{K}_{ab} = -[T_{\mu\nu}n^\mu n^\nu] \tag{2·10}$$

and

$$S^b_{a|b} = -[T_{\mu\nu}\tilde{h}_a{}^\mu n^\nu] \, , \tag{2·11}$$

where

$$\tilde{K}_{ab}=\frac{1}{2}(K_{ab}^{+}+K_{ab}^{-}) \tag{2·12}$$

and

$$[A]=A^{+}-A^{-}.$$

The relations (2·7), (2·10) and (2·11) are basic equations for a shell motion and they were obtained first by Israel.[1] Here, we note that the gravitational constant G has apparently dropped out in (2·10) and (2·11). And, if we take weak gravity limit $G\to 0$ or $GS_{ab}\to 0$ with finite S_{ab}, the relation (2·7) gives $K_{ab}^{+}=K_{ab}^{-}\equiv K_{ab}$ and the relation (2·10) reduces to

$$S^{ab}K_{ab}=-[T_{\mu\nu}n^{\mu}n^{\nu}]. \tag{2·13}$$

Therefore, the relations (2·13) and (2·11) are found not to relate to the Einstain equation. It has been pointed out that these relations are nothing but an energy-momentum conservation, that is, $T^{\mu}_{z;\mu}=0$ reduces to (2·13) and $T^{\mu}_{a;\mu}=0$ does to (2·11).[9]

In a sense, the limit $G=0$ implies the flat spacetime. However, we can consider such an approximation where the curved background metric is not affected by the presence of the shell. For this "test shell case", the basic relations are given by (2·13) and (2·11). An example of the difference between the exact treatment and the test shell treatment will be discussed in § 4.

§ 3. Metric junction and a positive energy condition

Hereafter, we consider the motion of a spherical shell. The form of extrinsic curvature for this case is given in the Appendix.

As Berezin, Kuzmin and Tkachev discussed,[5] we can use one of the relations (2·7) as a "necessary" condition for the metric junction. We require that the surface energy density of the shell should be positive, that is

$$K_{2}^{2+}-K_{2}^{2-}=4\pi GS_{0}^{0}\geq 0. \tag{3·1}$$

This condition is applicable only for the timelike hypersurface Σ. For the spacelike Σ, see Ref. 5).

Now, we examine the metric junction among the Minkowski metric (M), the Schwarzschild metric (S) and the positively curved uniform space (C). Although we will consider in the later sections only the de Sitter metric (DS) as an example of the metric C, the result of this section is valid for other types of C.

The σ in (A·3) and (A·4) is always +1 for M but can be ±1 for S and C. For the cases we consider the relation $0\leq e^{-\lambda}\leq 1$ holds. It is concluded from (3·1) that the M-M junction is possible only if $GS_{0}^{0}=0$. Likewise, the S-M and the DS-M junctions are impossible. In the above notations like DS-M, the inner space where the center of spherical symmetry exists is written in the left.

For other junctions, we list them up in Fig. 1, with schematic pictures. The cases excluded by (3·1) are also given for completeness. The junction DS-S and DS-DS were discussed in Refs. 4) and 5) but the dynamics has not been discussed explicitly.

The above junctions chosen by (3·1) do not necessarily satisfy other equations of

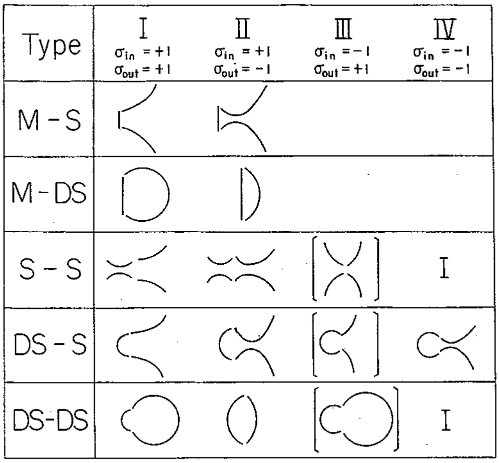

Fig. 1. Metric junctions among the Minkowski metric (M), the Schwarzschild metric (S) and the de Sitter metric (DS). The inner space where the center of spherical symmetry exists is written in the left like M("inner")-S("outer"). For each junction between the metrics, further differences specified by $\sigma_{\rm in}$ and $\sigma_{\rm out}$ are classified into types I ~IV. For each case, schematic pictures of the metric junction are given, where the "inner" space is written in the left.

The positive energy condition of the shell, (3·1), excludes some junctions like M-M, S-M and DS-M, those are not shown here. The type III cases drawn in the bracket [ ] are also excluded by the condition (3·1).

motion, which we will discuss in the following sections. We also mention that the above junctions are parts of multiple junctions, such as the case considered in Ref. 2).

§ 4. Motion of a dust shell in the vacuum

From (2·11), $S_0{}^0$ obeys the relation

$$\frac{dS_0{}^0}{d\tau}+2\frac{\dot{\rho}}{\rho}(S_0{}^0-S_2{}^2)=0\,. \tag{4·1}$$

For dust shell $S_0{}^0\neq 0$ and $S_2{}^2=0$ and $S_0{}^0\rho^2=\text{const}$.

(a) *The Minkowski-Schwarzschild junction*

We consider the M-S junction in Fig. 1. Using (A·4) and (A·5), we can write down (3·1) and (2·10) as

$$\sqrt{\dot{\rho}^2+1}-\sigma_{\rm out}\sqrt{\dot{\rho}^2+1-r_g/\rho}=4\pi G S_0{}^0\rho\,, \tag{4·2}$$

$$\frac{\ddot{\rho}}{\sqrt{\dot{\rho}^2+1}}+\sigma_{\rm out}\frac{\ddot{\rho}+(e^{-\lambda})^{\cdot}/2}{\sqrt{\dot{\rho}^2+1-r_g/\rho}}=0\,, \tag{4·3}$$

respectively. Multiplying (4·3) by $\dot{\rho}$, we can integrate once but the integration constant is determined uniquely by (4·2). Thus, we get

$$\sqrt{\dot{\rho}^2+1}+\sigma_{\rm out}\sqrt{\dot{\rho}^2+1-r_g/\rho}=r_g/Gm_s\,, \tag{4·4}$$

where $m_s\equiv 4\pi S_0{}^0\rho^2$ is the parameter specifying the shell. The sum of (4·2) and (4·4) gives

$$\sqrt{\dot{\rho}^2+1}-\frac{Gm_s}{2\rho}=\frac{m_g}{m_s} \tag{4·5}$$

with $m_g\equiv r_g/2G$.

If we write the metric of M as

$$ds^2=dT^2-dR^2-R^2d\Omega^2\,, \tag{4·6}$$

the proper time τ in (A·2) relates to T as $d\tau^2=\{1-(dR/dT)^2\}dT^2$ and $(dR/dT)=(d\tau/dT)\dot{\rho}$ $=\dot{\rho}/\sqrt{\dot{\rho}^2+1}$. Thus, the relation (4·5) is rewritten also

$$m_s\left(\frac{1}{\sqrt{1-(dR/dT)^2}}-1\right)-\frac{1}{2}\frac{Gm_s^2}{R}=-(m_s-m_g)\,.$$

The second term on the left-hand side is interpreted as a gravitational self-energy of the shell. If $m_s>m_g$, the maximum radius is obtained from (4·5) as

$$\rho_{\max}=\frac{Gm_s^2}{2(m_s-m_g)}\,. \tag{4·7}$$

It $m_s<m_g$, ρ can take any values.

Subtracting (4·2) from (4·5), we get

$$2\sigma_{\text{out}}\sqrt{\dot\rho^2+1-r_g/\rho}=(2m_g/m_s-Gm_s/\rho)\,. \tag{4·8}$$

Then, $\sigma_{\text{out}}\gtrless 0$ for $2m_g\rho\gtrless Gm_s^2$ respectively. Allowed region of motion on the ρ-(m_s/m_g) diagram is depicted in Fig. 2. As seen from this figure, the case of $m_g<m_s<2m_g$ corresponds to the type I junction in Fig. 1 and the case of $m_s>2m_g$ does to the type II junction. For $m_s=2m_g$, $\rho_{\max}=r_g$ and the both cases coincides.

The gravitational self-energy of the shell, $Gm_s^2/2\rho$, at $\rho_{\max}$ is computed as

$$\frac{Gm_s^2/2\rho_{\max}}{m_s}=1-\frac{m_g}{m_s}\,. \tag{4·9}$$

We notice from (4·7) that there are two different limiting values of m_s which gives $\rho_{\max}\to\infty$, those are A: $m_s\to m_g$ and B: $m_s\gg m_g$. In Case A which is included in the type I junction, the self-energy of (4·9) reduces to zero in this limit. But, in Case B which is included in the type II, the self-energy tends to m_s in this limit. Therefore, the Newtonian shell limit is found to be included in the type I. The type II junction does not reduce to the Newtonian limit even in the limit $\rho_{\max}\gg r_g$. Thus, the difference of junctions is connected to that of the self-energy.

In the test shell approximation, we should use (2·13) instead of (2·10). Then, from $S_0{}^0K_0{}^0=0$, we get

$$\dot\rho^2+1-r_g/\rho=C\,, \tag{4·10}$$

where C is an integration constant and is a free parameter different from the exact treatment. Equation (4·10) is nothing but a geodesic equation of a test particle and does not depend on m_s different from (4·5).

(b) *The Schwarzschild-Schwarzschild junction*

We consider the dust shell at the S-S junction in Fig. 1. Corresponding to (4·2) and (4·4), the basic equations are

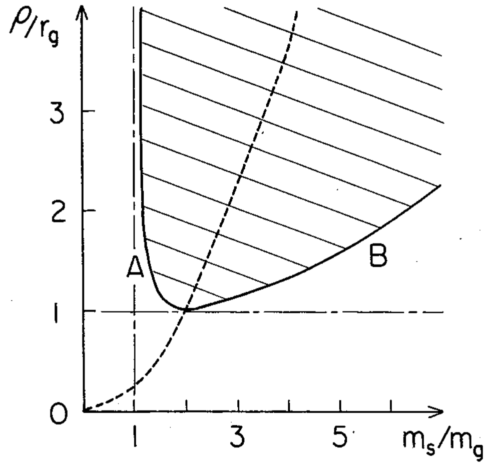

Fig. 2. For the dust shell at the Minkowski-Schwarzschild junction, allowed region of motion on the ρ-(m_s/m_g) diagram is given. The bold line shows $\rho_{\max}$ and the hatched region is a forbidden region of motion. The dotted line denotes $\rho/r_g=(m_s/m_g)^2/4$, which separates the sign of σ_{out}. The branch A is included in the type I junction and the B does in the type II. This figure as well as Fig. 3 has a meaning only for $\rho\ge r_g$.

$$\sigma_{\rm in}\sqrt{\dot\rho^2+1-r_{g1}/\rho}-\sigma_{\rm out}\sqrt{\dot\rho^2+1-r_{g2}/\rho}=\frac{Gm_s}{\rho} \tag{4·11}$$

and

$$\sigma_{\rm in}\sqrt{\dot\rho^2+1-r_{g1}/\rho}+\sigma_{\rm out}\sqrt{\dot\rho^2+1-r_{g2}/\rho}=\frac{r_{g2}-r_{g1}}{Gm_s}\,. \tag{4·12}$$

It is checked that $\sigma_{\rm in}\gtrless 0$ for $(r_{g2}-r_{g1})+G^2m_s{}^2/\rho\gtrless 0$ and $\sigma_{\rm out}\gtrless 0$ for $(r_{g2}-r_{g1})-G^2m_s{}^2/\rho\gtrless 0$. For $r_{g2}>r_{g1}$, $\sigma_{\rm in}>0$ always since $\rho>0$. The case $\sigma_{\rm out}>0$ corresponds to the type II junction in Fig. 1 and the case $\sigma_{\rm out}<0$ does to the type I. For $r_{g2}<r_{g1}$, $\sigma_{\rm out}<0$ always. The case $\sigma_{\rm in}<0$ corresponds to the type II and the case $\sigma_{\rm in}>0$ does to the type I.

From (4·11) and (4·12), the maximum radius is obtained as

$$\rho_{\rm max}=\frac{Gm_s{}^2}{2\{m_s-(m_1+m_2)\}}\,, \tag{4·13}$$

if $m_s>m_1+m_2$. Here, $m_i=r_{gi}/2G$. For $m_s<m_1+m_2$, ρ takes any values. The self-energy at $\rho_{\rm max}$ is computed as

$$\frac{Gm_s{}^2/2\rho_{\rm max}}{m_s}=1-\frac{m_1+m_2}{m_s}\,. \tag{4·14}$$

As in (4·9), these are two limits of $\rho_{\rm max}\to\infty$; (A) $m_s\to(m_1+m_2)$ and (B) $m_s\gg(m_1+m_2)$. Case A is included in the type II. The case of the type I junction reduces to the Newtonian limit in $\rho_{\rm max}\to\infty$.

§ 5. Vacuum-energy shell

The energy-momentum tensor of vacuum energy is characterized by $T_\mu{}^\nu=\varepsilon\delta_\mu{}^\nu/2$ and, for a spherical shell problem, it becomes $S_0{}^0=S_2{}^2=$constant as seen from (4·1).

For the class of metrics given by (A·6), the basic equations are

$$2\sigma_{\rm in}\sqrt{\dot\rho^2+e^{-\lambda_{\rm in}}}=A+B \tag{5·1}$$

and

$$2\sigma_{\rm out}\sqrt{\dot\rho^2+e^{-\lambda_{\rm out}}}=A-B\,, \tag{5·2}$$

where

$$A=(e^{-\lambda_{\rm in}}-e^{-\lambda_{\rm out}})/4\pi GS_0{}^0\rho \tag{5·3}$$

and

$$B=4\pi GS_0{}^0\rho\,. \tag{5·4}$$

(a) *Flat space with phase transition*[5)]

Putting $G=0$, $e^{-\lambda_{\rm in}}=e^{-\lambda_{\rm out}}=1$, $B=0$ but

$$A=\frac{2}{3}\frac{\Delta\varepsilon}{S_0{}^0}\rho\,,$$

where

$$\Delta\varepsilon \equiv \varepsilon_{\mathrm{out}} - \varepsilon_{\mathrm{in}} > 0 .$$

If we use the coordinates (4·6), the dynamic equation reduces to

$$\frac{4\pi R^2 S_0{}^0}{\sqrt{1-(dR/dT)^2}} - \frac{4\pi}{3}\Delta\varepsilon R^3 = 0 . \tag{5·5}$$

This relation is just an energy conservation for the sum of the latent energy generated by the phase transition and the kinetic energy of the shell.

The shell expansion in this case is solved as

$$\rho = \frac{1}{\alpha} \cosh \alpha\tau \tag{5·6}$$

with

$$\alpha = \frac{\Delta\varepsilon}{3S_0{}^0} . \tag{5·7}$$

(b) *The Minkowski-de Sitter junction*

We consider the M-DS junction in Fig. 1 with the vacuum-energy shell, putting $e^{-\lambda_{\mathrm{in}}}=1$ and $e^{-\lambda_{\mathrm{out}}}=1-8\pi G\varepsilon r^2/3$. Through the analysis like that for the previous cases, it is found that the type I and the type II junctions correspond to the case of $S_0{}^0 < S_{\mathrm{cr}}$ and $S_0{}^0 > S_{\mathrm{cr}}$ respectively, with

$$S_{\mathrm{cr}} \equiv \sqrt{\varepsilon/6\pi G} . \tag{5·8}$$

The shell motion is obtained as

$$\rho = \frac{1}{\alpha} \cosh \alpha\tau \tag{5·9}$$

with

$$\alpha = \frac{1}{3}\frac{\varepsilon}{S_0{}^0} + 2\pi G S_0{}^0 , \tag{5·10}$$

which takes the minimum at $S_0{}^0 = S_{\mathrm{cr}}$ as

$$\min\{\alpha\} = \sqrt{8\pi G\varepsilon/3} \equiv \alpha_{\mathrm{DS}} , \tag{5·11}$$

α_{DS} being the expansion rate of the de Sitter space. Here, we must note that τ is the proper time of the shell and is different from the comoving time in the de Sitter space.

(c) *The de Sitter-de Sitter junction*

We consider the DS-DS junction in Fig. 1, putting $e^{-\lambda_{\mathrm{in}}}=1-8\pi G\varepsilon_{\mathrm{in}} r^2/3$ and $e^{-\lambda_{\mathrm{out}}}=1-8\pi G\varepsilon_{\mathrm{out}} r^2/3$. If $|\varepsilon_{\mathrm{out}}+\varepsilon_{\mathrm{in}}| > 6\pi G S_0{}^{02}$, the junction is the type I in Fig. 1 and, if $|\varepsilon_{\mathrm{out}}+\varepsilon_{\mathrm{in}}| < 6\pi G S_0{}^{02}$, that is the type II. The expansion is given by

$$\rho = \frac{1}{\alpha} \cosh \alpha\tau \tag{5·12}$$

with

$$\alpha = \frac{\varepsilon_{\mathrm{in}} + \varepsilon_{\mathrm{out}}}{3S_0{}^0} + 2\pi G S_0{}^0 . \tag{5·13}$$

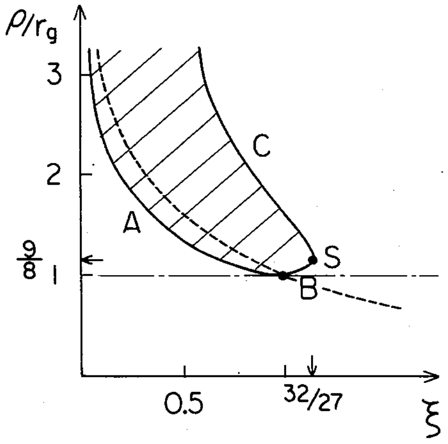

Fig. 3. For the vacuum energy shell at the Minkowski-Schwarzschild junction, allowed region of motion on the ρ-ξ diagram, being defined by (5·15). The bold line denotes ρ_0 and the hatched region is a forbidden region of motion. The dotted line denotes $(\rho/r_g)^3\xi^2=1$, which separates the sign of σ_{out}. The branch A is included in the type I junction and the branches B and C are done in the type II. The point S ($\xi=32/27$, $\rho=(9/8)r_g$) denotes an unstable static solution.

For varying $S_0{}^0$, α takes the minimum for $|\varepsilon_{\text{out}}+\varepsilon_{\text{in}}|=6\pi GS_0{}^{02}$ and

$$\min\{\alpha\}=\sqrt{\alpha^2_{\text{DS in}}+\alpha^2_{\text{DS out}}}\,. \tag{5·14}$$

(d) *The Minkowski-Schwarzschild junction*

We consider the M-S junction with the vacuum energy shell, putting $e^{-\lambda_{\text{in}}}=1$ and $e^{-\lambda_{\text{out}}}=1-r_g/r$. From (5·1), it is found that $\sigma_{\text{out}}\gtrless 0$ for $\xi^2(\rho/r_g)^3\lessgtr 1$ respectively, with

$$\xi\equiv 4\pi GS_0{}^0 r_g\,.$$

The radius ρ_0 obtained by putting $\dot\rho=0$ in the dynamic equation is the roots of

$$\xi^2\rho_0{}^3-2\xi r_g\rho_0{}^2+r_g{}^3=0\,. \tag{5·15}$$

The relation between ρ_0 and ξ is schematically depicted in Fig. 3. There exist two positive roots of ρ_0 if $0<\xi<32/27$. One of them describes the maximum trapped radius, which is either the branch A or B in Fig. 3. Another root describes the minimum bouncing radius, which is the branch C in Fig. 3. The branch A is included in the type I junction and the branches B and C are included in the type II. For $\xi\geq 32/27$, the junction is the type II. The point S in Fig. 3, where $\rho=(9/8)r_g$ and $\xi=32/27$, is an unstable static solution.

The inflation to $\rho\to\infty$ is possible only for the type II junction and ρ asymptotically increases as $\exp(\alpha\tau)$ with

$$\alpha=2\pi GS_0{}^0\,. \tag{5·16}$$

(e) *The de Sitter-Schwarzschild junction*

We consider the DS-S junction in Fig. 1, putting $e^{-\lambda_{\text{in}}}=1-8\pi G\varepsilon r^2/3$ and $e^{-\lambda_{\text{out}}}=1-r_g/r$. The relations (5·1) and (5·2) become

$$2\sigma_{\text{in}}\sqrt{\dot\rho^2+e^{-\lambda_{\text{in}}}}=\frac{r_g}{2\pi GS_0{}^0\rho^2}+\left(4\pi GS_0{}^0-\frac{2\varepsilon}{3S_0{}^0}\right)\rho \tag{5·17}$$

and

$$2\sigma_{\text{out}}\sqrt{\dot\rho^2+e^{-\lambda_{\text{out}}}}=\frac{r_g}{2\pi GS_0{}^0\rho^2}-\left(4\pi GS_0{}^0+\frac{2\varepsilon}{3S_0{}^0}\right)\rho\,. \tag{5·18}$$

The cases which inflate till $\rho\to\infty$ are included only for $\sigma_{\text{out}}<0$ as seen from (5·18). Therefore, the type I junction is excluded from such cases. From (5·17), it is found that the type II is for $4\pi GS_0{}^0>2\varepsilon/3S_0{}^0$ and the type IV for $4\pi GS_0{}^0<2\varepsilon/3S_0{}^0$.

The asymptotic expansion rate is given as

$$\alpha=\frac{\varepsilon}{3S_0{}^0}+2\pi GS_0{}^0\,, \tag{5·19}$$

which is the same as (5·10). And, the type IV for $S_0{}^0<S_{cr}$ and the type I for $S_0{}^0>S_{cr}$, S_{cr} being defined by (5·8).

§ 6. Discussion

We have checked all the possible junctions among M, S and DS, without appealing any intuitive interpretation and application. Interesting new result is that the type of junction is determined by the parameter of shell such as m_s or $S_0{}^0$. Therefore, it is anticipated that the different junction corresponds to different dynamical situation. However, an intuitive physical interpretation is not so clear. For example, the exclusion of all the type III junction by the positive energy condition is striking but is not obvious from the beginning.

The Newtonian limit is possible only for the M-S junction both for dust and vacuum-energy shells. So, we have investigated these cases rather in details in §§ 4 and 5(d). Particularly, the dust shell problem is the most easily conceivable case. Therefore, our nontrivial result is really unexpected one. Since the types I and II correspond dynamically different situations as seen in the self-energy of shell, they cannot be identified. So, if we try to recover our naive intuition, we have to find some other condition to exclude the type II juction. If such a condition were found, our result would be used to limit the shell parameter for "physical" situation. Anyhow, the type II case presents a new problem.

For the cases other than the M-S, our intuition is not so sound and all the types look equally reasonable!

Acknowledgements

The author thanks W. Israel for discussion. This study was initiated through the talks with him.

Appendix

—— *Extrinsic Curvature of Spherical Shell* ——

Spherically symmetric spacetime is written as

$$ds^2=e^{\nu}dt^2-e^{\lambda}dr^2-r^2d\Omega^2 \tag{A·1}$$

with $\nu(r,t)$, $\lambda(r,t)$ and $d\Omega^2=d\theta^2+\sin^2\theta d\varphi^2$. The metric of the hypersurface Σ, which is an evolutionary locus of the spherical shell, is written as

$$dl^2=d\tau^2-\rho(\tau)^2d\Omega^2\,, \tag{A·2}$$

where τ is the proper time of the shell and $4\pi\rho^2$ is a surface area. Due to the spherical symmetry, $S_2{}^2=S_3{}^3$ and $K_2{}^2=K_3{}^3$, where we take as $a=0, 2, 3$ for τ, θ, φ, respectively.

For the metric form of (A·1), the extrinsic curvature is computed as[5)]

$$K_0{}^0=-\sigma\left[\frac{\ddot\rho+\dot\rho^2(\lambda_{,r}+\nu_{,r})/2+\nu_{,r}e^{-\lambda}/2}{\sqrt{\dot\rho^2+e^{-\lambda}}}+\lambda_{,t}\dot\rho e^{(\lambda-\nu)/2}\right] \tag{A·3}$$

and

$$K_2{}^2 = -\sigma\frac{\sqrt{\dot{\rho}^2+e^{-\lambda}}}{\rho}, \tag{A$\cdot$4}$$

where $\dot{\rho}=d\rho/d\tau$, $\lambda_{,t}=\partial\lambda/\partial t$ and $\lambda_{,r}=\partial\lambda/\partial r$. If the spherical surface area increases with radial coordinate, $\sigma=1$ and $\sigma=-1$ otherwise.

If ν and λ do not depend on t, the relation $\nu+\lambda=0$ holds and the expression of $K_0{}^0$ reduces to a simple form of

$$K_0{}^0 = -\sigma\frac{\ddot{\rho}+(e^{-\lambda})_{,r}/2}{\sqrt{\dot{\rho}^2+e^{-\lambda}}}. \tag{A$\cdot$5}$$

The Schwarzschild-de Sitter metric of

$$e^{\nu}=e^{-\lambda}=1-\frac{r_g}{r}-\frac{8\pi}{3}G\varepsilon r^2 \tag{A$\cdot$6}$$

belongs to this category.

The dust universe model treated in Ref. 2) does not belong to this category. In the text, we study only the metrics whose $K_0{}^0$ reduces to (A$\cdot$5).

References

1) W. Israel, Nuovo Cim. **44B** (1966), 1; **48B** (1967), 463.
V. De La Cruz and W. Israel, Nuovo Cim. **51A** (1967), 744.
2) K. Sato, M. Sasaki, H. Kodama and K. Maeda, Prog. Theor. Phys. **65** (1981), 1443.
K. Maeda, K. Sato, M. Sasaki and H. Kodama, Phys. Lett. **108B** (1982), 98.
3) Z. Ch. Wu, Phys. Rev. **D28** (1983), 1898.
4) V. A. Berezin, V. A. Kuzmin and I. I. Tkachev, Phys. Lett. **120B** (1983), 91.
5) V. A. Berezin, V. A. Kuzmin and I. I. Tkachev, Phys. Lett. **130B** (1983), 23; JETP Lett. **40** (1985), 547.
6) H. Sato, in *General Relativity and Gravitation,* ed. B. Bertotti et al. (D. Reidel Pub. Comp., 1984), p. 239.
7) K. Maeda and H. Sato, Prog. Theor. Phys. **70** (1983), 772, 1276.
8) S. Ikeuchi, K. Tomisaka and J. P. Ostriker, Astrophys. J. **265** (1983), 583.
9) V. A. Berezin, V. A. Kuzmin and I. I. Tkachev, Sov. Phys.-JETP **59** (1984), 459; Phys. Lett. **124B** (1983), 479.

Note added: The author found that some results in § 4 have been obtained in the papers, M. A. Markov and V. P. Frolov, Teori. Mat. Phys. **3** (1970), 3 and V. P. Frolov, JETP **66** (1974), 813. He thanks V. P. Frolov for pointing out this.